Journal of Polymer Research (2022) 29: 319
https://doi.org/10.1007/s10965-022-03184-2

ORIGINAL PAPER

Large-scale preparation of polylactic acid/polyethylene glycol micro/nanofiber fabrics with aligned fibers via a post-drafting melt blown process

Huan-Wei Sun[1,2,3] · Heng Zhang[1,2,3] · Qi Zhen[1,2,3] · Si-Fan Wang[1,2,3] · Jun-Jie Hu[4] · Jing-Qiang Cui[4,6] · Xiao-Ming Qian[3,5]

Received: 6 April 2022 / Accepted: 5 July 2022 / Published online: 11 July 2022

Abstract

Polylactic acid (PLA) micro/nanofiber fabrics with good biodegradability and biocompatibility have wide applications in the medical protective field. However, the poor flexibility, high brittleness, and insufficient mechanical properties of PLA micro/nanofiber fabrics remain challenging. Herein, a polylactic acid/polyethylene glycol (PLA/PEG) micro/nanofiber fabric with aligned fibers was successfully prepared by an inexpensive and straightforward post-drafting melt blown process. The experimental results showed that PEG can reduce the T_g of PLA, improve the mobility of PLA molecular chains, reduce the complex viscosity of PLA/PEG blends, and play a role in plasticization. The PLA/PEG micro/nanofiber fabrics had an aligned micro/nanofibrous structure, and the average fiber diameter was easily adjusted from 10.7 to 4.9 μm by tailoring the melt blown process parameters, i.e., die temperature and hot air temperature. Moreover, the breaking tensile strength increased from 45.06 to 78.73 N in the machine direction (MD), while it increased from 11.87 to 21.89 N in the cross direction (CD), which means that the breaking tensile strength was enhanced significantly by adjusting the die temperature and hot air temperature. Furthermore, the prepared samples showed a high softness score of 82.7, a large synthetic blood contact angle of 125.7°, and an excellent bursting strength of 58.5 N. These PLA/PEG micro/nanofiber fabrics with aligned fibers are ideal candidates for medical protective applications such as surgical gowns, protection suits, masks, and medical bandages.

Keywords Micro/nanofibers · Melt blown · Polylactic acid · Biodegradable · Nonwoven

✉ Heng Zhang
m-esp@163.com; zhangheng2699@zut.edu.cn

1 School of Textile, Zhongyuan University of Technology, Xinzheng County, No. 1 Huaihe RoadHenan Province, Zhengzhou 451191, China

2 School of Clothing, Zhongyuan University of Technology, Xinzheng County, No. 1 Huaihe RoadHenan Province, Zhengzhou 451191, China

3 Henan Key Laboratory of Medical Polymer Materials Technology and Application, Changyuan County, No. 1 Yangze RoadHenan Province, Xinxiang 453400, China

4 Shanghai Earntz Nonwoven Co, Jinshan District, Jiangong Road, LtdShanghai 201501, No. 88, China

5 School of Textile Science and Engineering, Tiangong University, Xiqing District, No. 399 Binshui Xilu Road, Tianjin 300387, China

6 Henan Tuoren Medical Device CoTuoren Industrial Zone, Changyuan CountyChangyuan County, No. 1 Yangze RoadXinxiang Henan Province, Ltd 453400, China

Introduction

The melt blown process, one of the most widespread technologies for micro/nanofiber fabrics, has a series of attractive characteristics, such as large scale, no potential solvent toxicity, and abundant resources [1, 2]. In addition, melt blown fabrics composed of petroleum-based polymers, i.e., polypropylene (PP), polyethylene (PE), and polyester (PET) [3], have been widely used in personal hygiene, medical protection, packaging, filtration, separation, and other industries due to the cooperative advantages between the properties of micro/nanofibers and polymers [4–6]. However, there are problems in recycling and non-degradation, which has introduced severe pollution to the environment in recent years [7–9]. For example, the COVID-19 pandemic has driven explosive growth in the use of personal protective equipment (masks and protective clothing) made of PP micro/nanofiber fabrics, which has been improperly disposed of in

the ocean, soil, and sky, further aggravating risks to ecological systems [10].

Recently, polylactic acid (PLA) micro/nanofiber fabrics have become a trending research topic due to their good biodegradability and safety properties [11, 12]. Continued efforts have been made to develop commercial applications and large-scale preparations of PLA micro/nanofiber fabrics [13]. For instance, Feng [14] prepared PLA melt blown fabrics with biodegradable properties and researched the influence of the die-to-collector distance (DCD) on PLA fiber diameter, porosity, and stress. Hammonds et al. [15] investigated the effects of airflow and DCD on the physical and thermal properties of PLA melt blown fabrics with the aim of meeting specific requirements for tissue scaffolds. Łatwińska et al. [16] used biodegradable polymer PLA and nonbiodegradable polymer PP as raw materials to prepare melt blown fabrics and added $CuO{\cdot}SiO_2$ to induce antibacterial properties to apply filter materials. It is clear from the above research that PLA micro/nanofiber fabrics provide a viable option that replaces traditional PP fabrics. However, in the actual application process, PLA micro/nanofiber fabrics have the disadvantages of poor flexibility, high brittleness, and low mechanical properties during long-term storage [17, 18]. Therefore, it is important to improve the mechanical properties of PLA micro/nanofiber fabrics for their popularization and application.

To that end, blending is a convenient, efficient, and scalable technology for the melt blending process [19]. Scholars have begun to melt PLA and other polymers for melt blending molding to improve the mechanical properties of PLA melt blown nonwoven fabrics [20–22]. Polyethylene glycol (PEG) is an environmentally friendly material with the characteristics of commercialization, degradability, harmlessness to the human body, and good thermal stability [23]. As a suitable plasticizer, PEG can be melt-blended with PLA to improve the degradation rate, crystallization kinetics and mechanical properties of PLA [24–26]. Jiang et al. [27] used melt blending to add PEG to enhance the toughness and gas barrier properties of PLA for use in disposable packaging and agricultural films. Their results showed that adding 10 wt% PEG can greatly improve the toughness and gas barrier ability of PLA film without losing its film-blowing stability. Huang et al. [28] used a solid plasticizer (PEG) and a liquid plasticizer (epoxidized soybean oil, ESO) to modify PLA and successfully prepared different types of plasticizer-modified polylactic acid blends through melt blending. Therefore, it is strongly believed that blending PEG and PLA during the melt blown process would be an aggressive strategy for the large-scale preparation of polylactic acid/polyethylene glycol micro/nanofiber fabrics. However, to the best of our knowledge, the effect of the melt blown process on the structural and mechanical properties of PLA/PEG micro/nanofiber fabrics has rarely been reported.

Herein, PLA/PEG micro/nanofiber fabrics were prepared with aligned fibers via a post-drafting melt blown process, and the thermodynamic and rheological properties of the PLA/PEG blended polymer were investigated. Moreover, the influence of the melt blown process (die temperature and hot air temperature) on the structure and properties of the prepared samples was analyzed for various potential applications, such as surgical gowns, protection suits, masks, and medical bandages.

Materials and methods

Materials

PLA chips (6252D, Nature Works, USA) with a melting flow index of 85 g/10 min at 210 °C were purchased from Henan Tuoren Medical Device Co., Ltd. (Henan, China). The PEG chips (molecular weight = 6000, melting point = 54 ℃) were purchased from Jiangsu Haian Petroleum Chemical Factory (Jiangsu, China). The PLA chips were dried in a drying chamber at 80 °C for 8 h, and then blended with the PEG chips heated and melted by a water bath at 80 °C, so that the PEG was evenly wrapped on the surface of the PLA chips. The mass ratio of the PLA/PEG blended chips was 97:3.

Preparation

PLA/PEG micro/nanofiber fabrics were fabricated by a melt blown testing system (200A, Suzhou Doro New Materials Technology Co. LTD, China). A schematic diagram of the melt blown process is shown in Fig. 1. During the melt blown process, PLA/PEG blended chips were fed into a screw extruder, where the blended chips were melted into a blended melt and then extruded into a spinneret. The PLA/PEG blended melt passed through the spinneret orifice to form melt jets. Meanwhile, the melt jets were drawn by a high-speed hot air stream, resulting in the formation of PLA/PEG micro/nanofibers. Subsequently, the PLA/PEG micro/nanofibers were collected on the receiving webs to form PLA/PEG micro/nanofiber webs. Finally, a certain post-drafting force is applied to the PLA/PEG micro/nanofiber web through the difference between the speed of the collector (V1) and the speed of the drafting roller (V2) to realize the post-drafting of the PLA/PEG micro/nanofiber webs, thereby forming PLA/PEG micro/nanofiber fabrics with aligned fibers. For the melt blown testing system, the orifice diameter was 0.25 mm, and the post-drafting ratio was 2:1. The die temperature was set at 200–230 °C, while the hot-air temperature was set at 210–240 °C.

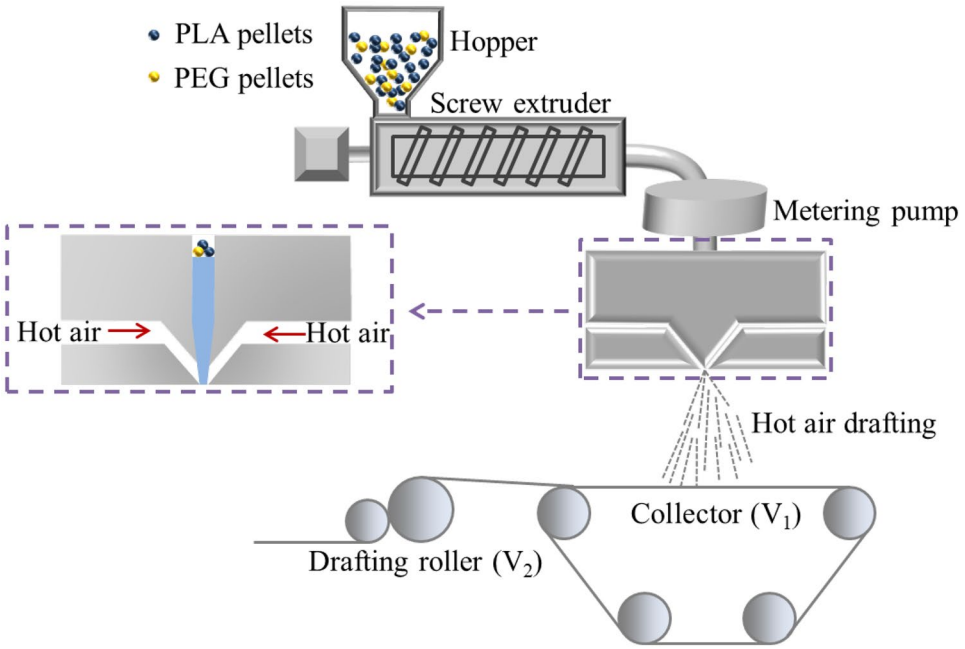

Fig. 1 Schematic of the preparation process of PLA/PEG micro/nanofiber fabrics via a post-drafting melt blown process

Characterizations

Blended polymer properties

The melting behavior, thermal stability, and rheological behavior of the pure PLA and PLA/PEG blended chip samples were characterized by a differential scanning calorimeter (DSC, DSC25, TA Instrument, USA), thermogravimetric analysis (TG, 209 F1 Libra®, NETZSCH, Germany), and a rheometer (ARES-RFS III, TA Instrument, USA), respectively. During the DSC testing, the melting rate was 10 ℃/min. For the TG testing, the scanning temperature was set at 30–600 °C at a heating rate under a nitrogen atmosphere. Moreover, rheological behavior was observed at shear rates ranging from 500 to 3000 s^{-1}, and the testing temperature was 190–230 ℃.

Morphology

The surface morphology of the prepared sample of PLA/PEG micro/nanofiber fabrics was analyzed by scanning electron microscopy (SEM, EVO18, ZEISS, Germany). In addition, fiber diameters and diameter distributions were analyzed by Nano Measurer software. Fifty fibers were measured for the fiber diameter measurement.

Mechanical performance

Stress–displacement curves of the samples clamped 50 *200 mm were tested using a fabric tensile tester (HD026S-100, Nantong Hongda experimental Instrument Co., Ltd, China) according to GB/T 24,218.3–2014(Textiles Test methods for nonwovens—Part 3: Determination of breaking strength and elongation at break (strip method)).

The bursting curve of the samples was tested using a testing machine (YG026MD, Wenzhou Fangyuan Instrument Co., Ltd, China) based on the GB/T 19,976–2005(Textiles Determination of bursting strength Steel ball method).

Softness and air permeability

Softness scores were determined using a softness tester (Phabr Ometer, Nu CyberTek, Inc., USA) according to AATCC TM 202–2014(Test Method for Relative Hand Value of Textiles: Instrumental).

Air permeability was tested using an air permeability tester (YG461E; Wenzhou Darong Textile Instrument, China) according to GB/T 5453–1997(Textiles Determination of the air permeability of fabrics).

Liquid contact angles (LCAs) and absorbability

LCA measurements were achieved by a contact angle system (SDC-350, Dongguan Shengding Precision Instruments Co., Ltd, China). The testing liquid was synthetic blood, and the composition was sodium carboxymethyl cellulose 2 g, amaranth 1 g, sodium chloride 4.5 g, and water (final volume) 1 L.

Results and discussions

Thermal properties

The DSC heating and cooling curves of PLA/PEG (100/0) and PLA/PEG (97/3) blends are shown in Fig. 2a. In the trace of the pure PLA heating curve, the glass transition temperature (T_g) was 61.6 ℃, and a cold crystallization temperature (T_{cc}) at 108.3 ℃ was observed due to the mobility and rearrangement of PLA macromolecules. Pure PLA displayed two prominent separated melting peaks (T_m) at 151.4 ℃ and 159.9 ℃, which could be explained by the mechanisms of melt recrystallization, multiple lamellae, or crystal structures [29, 30]. In the cooling process of pure PLA, no obvious crystallization peak (T_c) was found because of its slow crystallization rate [31]. With the addition of PEG, the T_g of PLA/PEG (97/3) decreased to 57.3 °C, which indicated that under the plasticizing action of PEG, the free volume of PLA molecular chains increased, and the movement ability of PLA molecular chains increased [26]. In addition, the addition of PEG reduced the T_{cc} from 108.3 °C to 103.2 °C. The decrease in T_{cc} proved that PEG had an excellent acceleration effect on the amorphous phase of PLA. The PLA molecules in the PLA/PEG chain can undergo cold crystallization at a lower temperature during the heating process, indicating that the PLA molecular chain has increased mobility and crystallization ability [23, 32]. However, during the cooling process, the addition of PEG still has no apparent cold crystallization peak.

Biodegradable polymers generally display poor thermal stability, which affects the processing and properties of the end product [33]. Figure 2b shows the weight as a function of temperature for pure PLA and PLA/PEG (97/3) blends. A single thermal degradation stage was observed in pure PLA and PLA/PEG (97/3). The initial thermal decomposition temperature ($_{Initial}$) of pure PLA was approximately 291.6 °C, the thermal decomposition interval of PLA was 312.6–367.1 °C, and the practical melt blown processing temperature was generally between 210–240 °C. After adding PEG, the initial and thermal decomposition intervals of PLA/PEG changed slightly, but the change was not noticeable. Related studies have shown that as the molecular weight of PEG is added, the thermal stability of PLA/PEG improves [34].

Rheological properties

All thermoplastic polymers could theoretically be applied to produce melt blown nonwoven materials, but the properties of the polymers, especially the melt viscosity, significantly affected the processing of melt blown technology [35]. The process dynamics and web structure of melt blown nonwoven materials were also influenced by the rheological properties of the melt [36]. The effect of shearing rates on the complex viscosity of the pure PLA and PLA/PEG (97/3) blends at 190–230 °C is shown in Fig. 3. It was obvious that the pure PLA and PLA/PEG (97/3) blends exhibited non-Newtonian "shear-thinning" behaviors, and the complex viscosity of the pure PLA and PLA/PEG blends decreased significantly with increasing shearing rates [37]. Figure 3 shows that as the temperature increases, the complex viscosity of the pure PLA and PLA/PEG blends decreases. As the temperature increases, the thermal motion of molecules intensifies, and the distance between molecules increases. More energy makes the molecules form more free bodies, the chain segments are easier to move, and the interaction between molecules is reduced. Therefore, the complex viscosity of the material decreases [38]. In comparing Fig. 3a and b, it can be seen that the complex viscosity of pure PLA is higher. With the addition of PEG, the complex viscosity of the composite material decreases, indicating that PEG has a better plasticizing effect on PLA [39, 40].

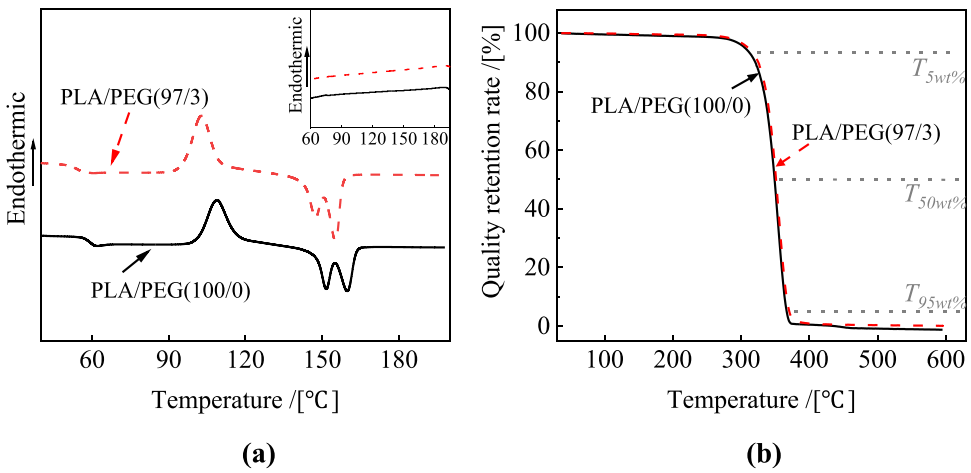

Fig. 2 DSC **a** and TG **b** curves of PLA/PEG (100/0) and PLA/PEG (97/3)

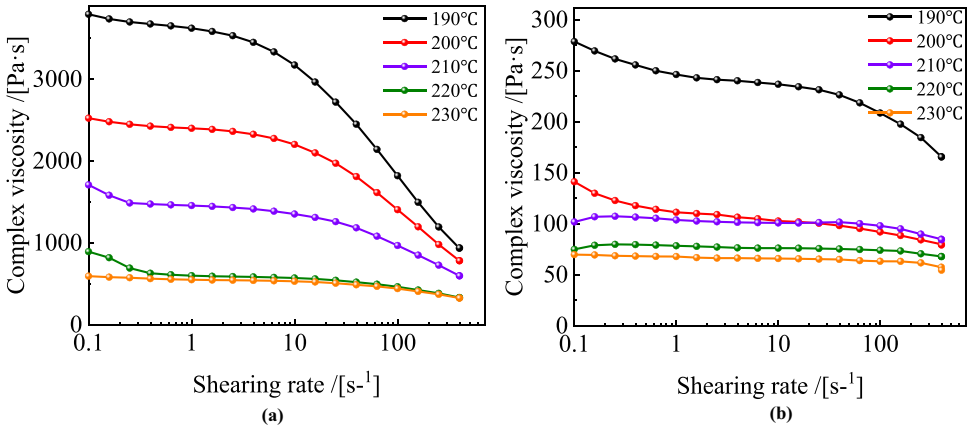

Fig. 3 Rheological property curves of PLA/PEG (100/0) **a** and PLA/PEG (97/3) **b** at different temperatures

Morphology and fiber diameter distribution

Figures 4 and 5 show the morphologies and fiber diameter distribution of PLA/PEG (97/3) micro/nanofiber fabrics with different die temperatures and hot air temperatures. It can be seen in the figure that the fabrics are formed by stacking micro/nanofibers of varying diameters in the thickness direction. Under the action of the post-drafting process, the fiber web will be subjected to a certain external force. At this time, the friction force between the fibers is less than the external force, and a large number of fibers are aligned along the drafting direction (longitudinal direction). Meanwhile, the fibers diameters are mainly distributed between 0.4 μm and 10.5 μm. With increasing die temperature and hot air temperature, the fiber gradually becomes thinner, and the peak value of the fiber diameter distribution moves forward. Figure 6 shows the maximum and average fiber diameters under different die temperatures and hot air temperatures. As shown in Fig. 6, as the die temperature increases to 230 °C, the average fiber diameter decreases from 10.7 μm to 5.3 μm. The hot air temperature increased to 240 °C, and the average fiber diameter decreased from 7.8 μm to 4.9 μm. The main reason for this phenomenon is that the increase in temperature can improve the fluidity of the PLA/PEG melt. After the melt is sprayed through the spinneret, the drawing will be more adequate under high-speed hot air drawing, so the fiber diameter decreases.

Mechanical properties

It is well known that melt blown nonwovens are made of ultrafine fibers bonded to each other, and have porous and fluffy structural characteristics. Both structures provide tensile strength to the melt blown nonwovens. When melt blown nonwovens undergo stretching, the tensile force first makes the fabric narrower, and fibers compress against each other. Subsequently, the tensile force is transmitted to the bonding points, and when the bearing capacity of the bonding points reachthe limit, the bonding points are forced to separate. An equilibrium phase usually occurs when tensile

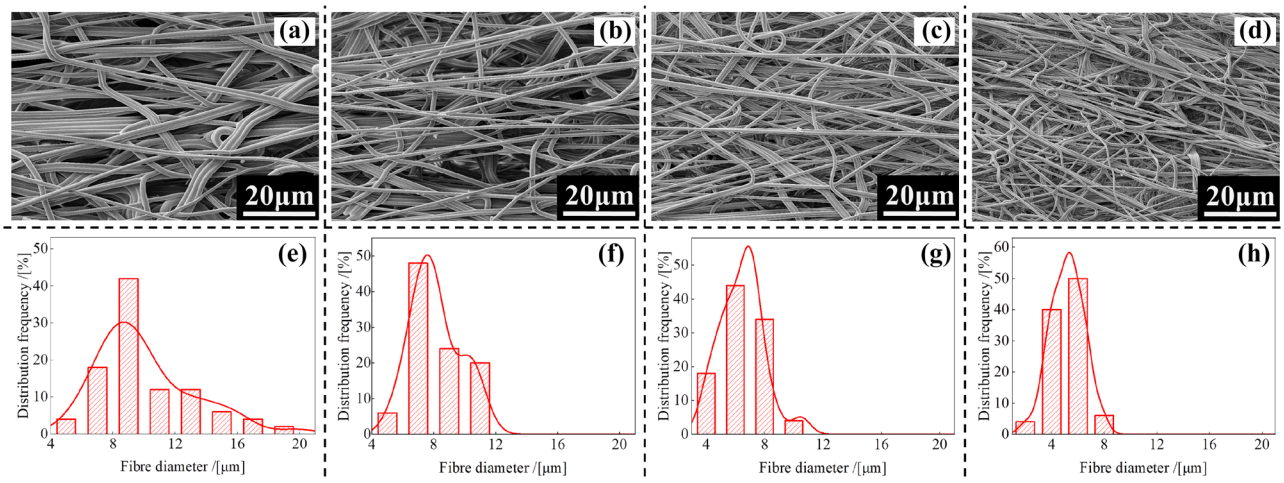

Fig. 4 **a-d** SEM images and **e–h** fiber diameter distributions of the sample surfaces at different die temperatures at a hot air temperature of 230 °C: **a**, e = 200 °C, **b**, f = 210 °C, **c**, g = 220 °C, **d**, h = 230 °C.

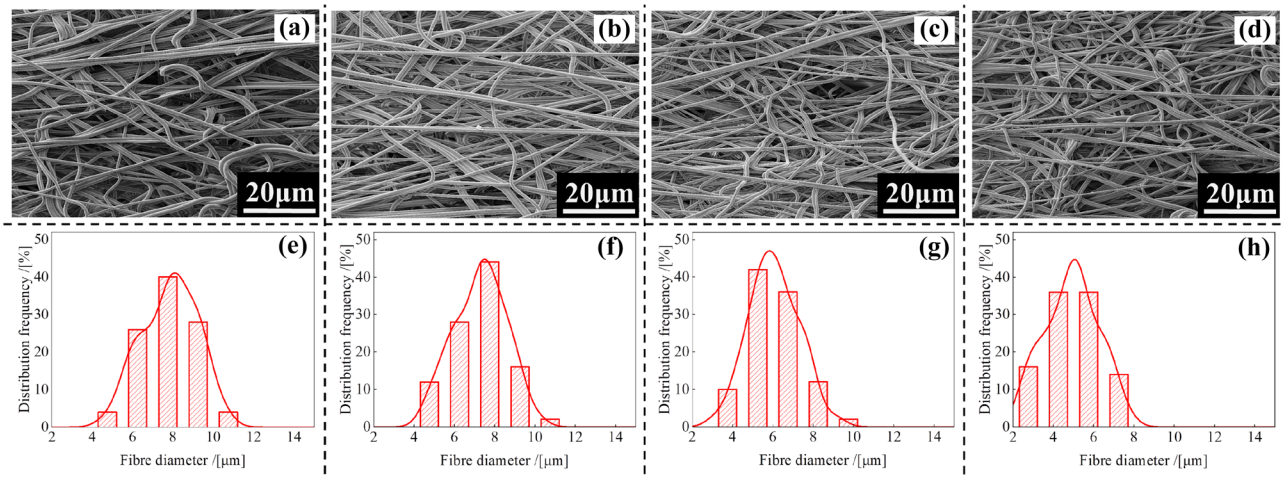

Fig. 5 **a-d** SEM images and **e-h** fiber diameter distributions of the sample surfaces at different hot air temperatures at a die temperature of 220 °C: **a**, e = 210 °C, **b**, f = 220 °C, **c**, g = 230 °C, **d**, h = 240 °C.

fracture of fibers and disintegration of bond points are balanced with contributions from new fibers and bond points. Finally, the melt blown web is destroyed, and the strength decreases [33]. In this experiment, the tensile strengths of PLA/PEG micro/nanofiber fabrics under different die temperatures and hot air temperature were explored under the condition that the areal density of PLA/PEG micro/nanofiber fabrics remained unchanged. As clearly shown in Figs. 7 and 8, the maximum stresses of the samples in the machine direction (MD) and cross direction (CD) gradually increased from 52.93 N to 67.58 N and increased from 11.92 N to 15.99 N with increasing die temperature, respectively. The maximum stresses of the samples gradually increased from 45.06 N to 78.98 N and increased from 12.01 N to 21.89 N with increasing hot air temperature, respectively. This phenomenon occurs because the rise in the die temperature and hot air temperature can improve the fluidity of the melt. Thus, the fiber is fully drawn, the fiber diameter is reduced, and the number of cross, entanglement, and bonding points between the fibers increases. Therefore, the overall fiber web strength increases. At the same time, the cross, entanglement, and bonding points between the fibers increase, making it difficult to break during the tensile fracture process, so the elongation at the break of the fabrics also gradually increases.

Figure 9 shows the bursting strength curves of PLA/PEG micro/nanofiber fabrics under different die temperatures and hot air temperatures. It can be seen in the figure that with the increase in the die temperature and hot air temperature, the bursting strength of the material gradually increases, and the maximum can reach 58.6 N. The reason is that as the temperature increases, the fiber diameter becomes thinner, and the cross, entanglement, and bonding points between the fibers increase, so the bursting strength increases. At the same time, the temperature rise makes the fiber draw more fully, promotes the crystallization of the fiber, and increases the strength of a single fiber, thereby improving the overall impact resistance of the fabrics.

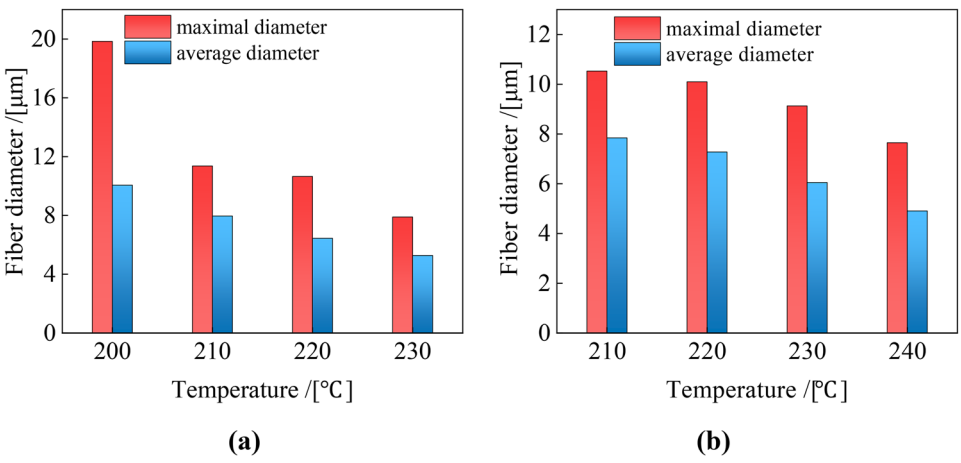

Fig. 6 Average fiber diameter and maximum fiber diameter of different process samples: **a** samples of different die temperatures and **b** samples of different hot air temperatures

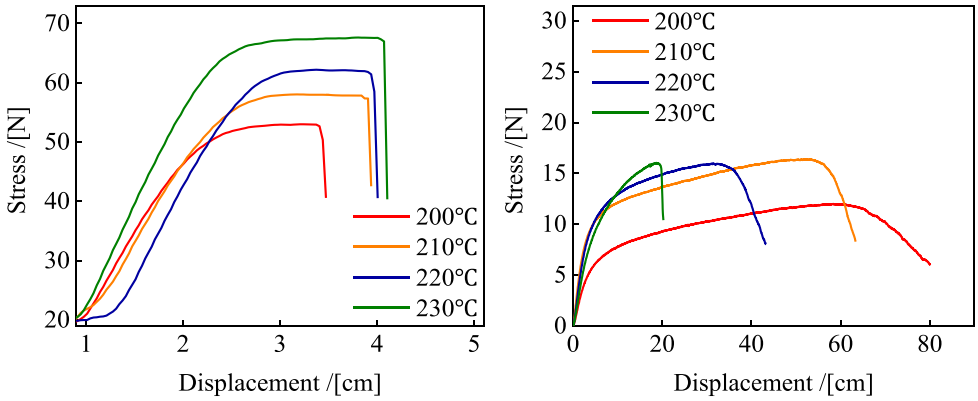

Fig. 7 Stress–displacement curves of the samples in **a** CD and **b** MD at different die temperatures

Comfort performance

The Phabr Ometer is a testing system that evaluates the sensory performance of fabrics in contact with human skin, and the softness scores are used to assess the softness properties of fabrics [41]. Figure 10a demonstrates the softness scores of the PLA/PEG micro/nanofiber fabrics with different die temperatures and hot air temperatures. Figure 10a summarizes the changes in softness scores of the fabrics prepared at different die temperatures and hot air temperatures. The softness scores increased from 69.82 to 78.62 as the die temperature increased from 200 ℃ to 230 ℃, and the softness scores increased from 76.34 to 82.70 as the hot air temperature increased from 210 ℃ to 240 ℃, showing excellent softness properties. The superior softness properties of the PLA/PEG micro/nanofiber fabrics were mainly attributed to small-fiber diameters on the micro/nanoscale and the fluffy structure from the interconnected "curved" fibers. Overall, based on these experimental results, high die temperatures and hot air temperatures improved the softness of the samples.

We also explored the effect of different die temperatures and hot air temperatures on the air permeability of PLA/PEG micro/nanofiber fabrics while ensuring the same areal density of the fabrics (Fig. 10b). It can be seen from the figure that the air permeability of samples with different die temperatures and hot air temperatures gradually decreased. As the die temperature increased from 200 to 230 °C, the air permeability of the sample decreased from 623.8 to 173.8 mm/s^{-1}. As the temperature of the hot air increased from 210 °C to 240 °C, the air permeability of the sample decreased from 351.4 mm/s^{-1} to 170.1 mm/s^{-1}. This may be because the number of fine fibers increased with increasing temperature, thus increasing the flow resistance.

Synthetic blood contact angles

Synthetic blood was dripped on the sample surface of the PLA/PEG micro/nanofiber fabrics to evaluate liquid wettability. Optical images (Fig. 11b) showed that the synthetic blood droplets on the surface of the samples always exhibited a nearly spherical shape, which indicates that the fabrics are hydrophobic, i.e., they are not wetted by blood and water. Figure 11a shows the change rule of the synthetic blood contact angle of the PLA/PEG micro/nanofiber fabrics with different melt blown processes. It can be seen in the figure

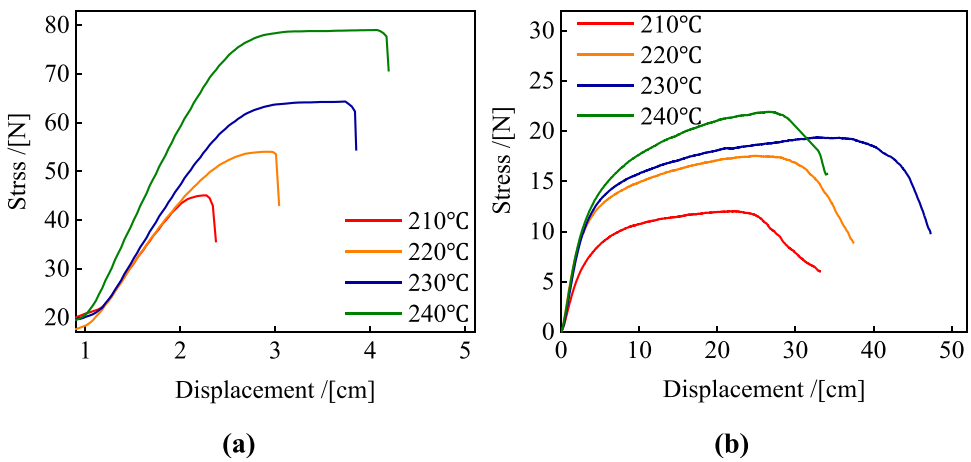

Fig. 8 Stress–displacement curves of the samples in **a** CD and **b** MD at different hot air temperatures

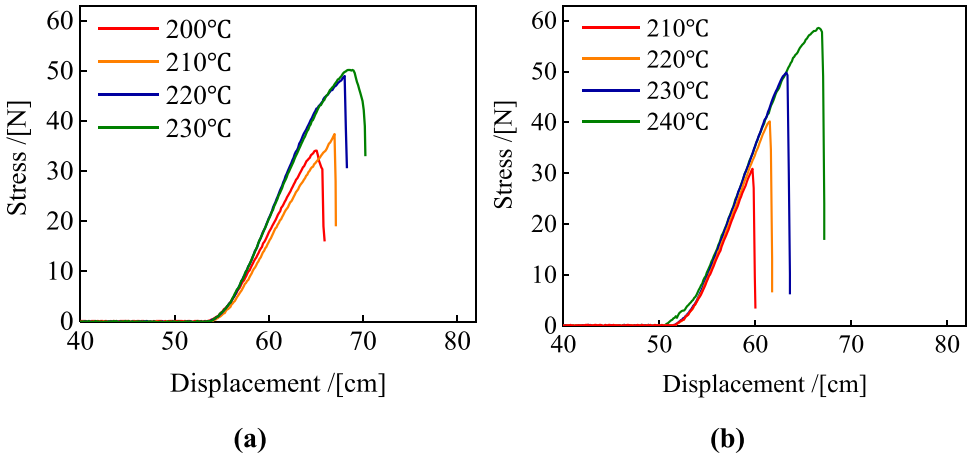

Fig. 9 Bursting strength of samples with different die temperatures **a** and hot air temperatures **b**

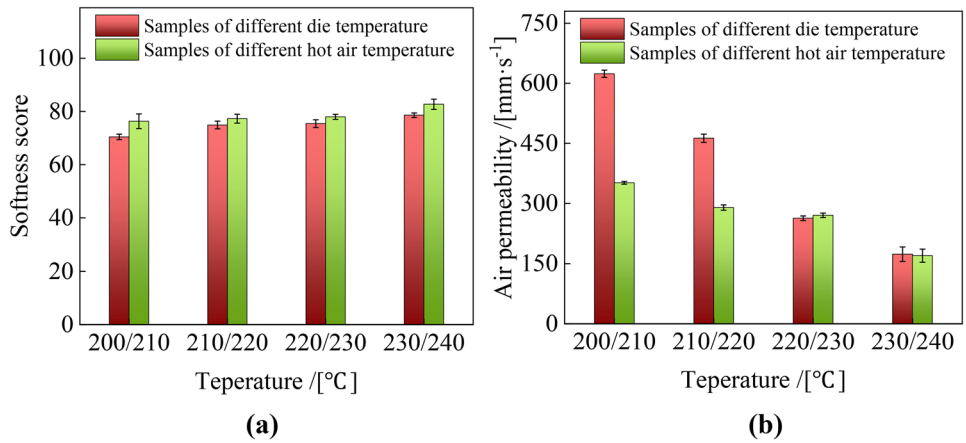

Fig. 10 Softness scores **a** and air permeability **b** of samples at different die and hot air temperatures

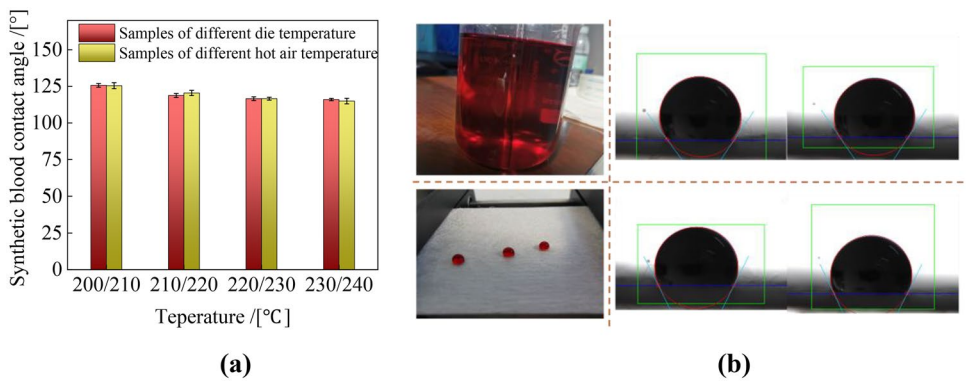

Fig. 11 Synthetic blood contact angles with different melt blown processes **a** Synthetic blood contact angles of samples with different die temperatures and hot air temperatures **b** Photographic images of the synthetic blood droplets on the surface of the PLA/PEG micro/nanofiber fabrics

that the synthetic blood contact angle of the sample is distributed between 115.0–125.7°. As the die temperature and hot air temperature increase, the sample's synthetic blood contact angle gradually decreases. The reason may be that the increase in the die temperature and hot air temperature fully stretches the fiber. The fiber diameter is reduced while reducing the roughness of the fiber surface, so the synthetic blood contact angle is reduced.

Conclusions

In this work, PLA/PEG micro/nanofiber fabrics were prepared with aligned fibers by a post-drafting melt blown process, and the effects of the melt blown process (die temperature and hot air temperature) on the structure and properties of PLA/PEG micro/nanofiber fabrics were analyzed. Thermodynamic analysis showed that the addition of PEG could improve the crystallization properties of PLA, thereby enhancing the mechanical properties of PLA. A dynamic rheological property test also verified that the PLA/PEG blend melt exhibited typical shear thinning. The composite viscosity of PLA/PEG melts decreased with increasing melt temperature, ranging from 190 to 230 ℃. With increasing die temperature and hot air temperature, the average diameter of the fibers decreased to 5.3 μm and 4.9 μm, respectively. The mechanical properties of the fabric gradually improved, and the softness scores were distributed between 69.82 and 82.7. Overall, the results of this study served as a valuable reference for the commercial application and large-scale preparation of PLA/PEG micro/nanofiber fabrics developed for various potential applications, especially for medical protectives such as surgical gowns, protection suits, masks, and medical bandages.

Supplementary Information The online version contains supplementary material available at https://doi.org/10.1007/s10965-022-03184-2.

Acknowledgements This work was supported by the National Natural Science Foundation of China (52003306), National Biomedical Material Production and Application Demonstration Platform of China (TC190H3ZV/1), Henan Key Laboratory of Medical Polymer Materials Technology and Application (1-TR-B-03-210117), and Zhongyuan University of Technology (K2020YY002).

Author contributions All Author contributed equally to this work.

Declarations

Conflicts of interest The authors declare that they have no known competing financial interests or personal relationships that could have appeared to influence the work reported in this paper.

References

1. Zhang HF, Liu JX, Zhang X et al (2018) Design of electret polypropylene melt blown air filtration material containing nucleating agent for effective PM2.5 capture. RSC Adv 8(15): 7932–7941. https://doi.org/10.1039/c7ra10916d
2. Kara Y, Molnár K (2021) Revealing of process–structure–property relationships of fine polypropylene fiber mats generated via melt blowing. Polym Adv Technol 32(6):2416–2432. https://doi.org/10.1002/pat.5270
3. Zhu FC, Su JJ, Zhao YH et al (2019) Influence of halloysite nanotubes on poly(lactic acid) melt-blown nonwovens compatibilized by dual-monomer melt-grafted poly(lactic acid). J Text Res 89(19–20):4173–4185. https://doi.org/10.1177/0040517519826926
4. Sun HW, Zhang H, Zhen Q et al (2020) Filtrations of propylene-based micro-nano elastic filters via melt blowing process. J Text Res 41(10):20–28. https://doi.org/10.13475/j.fzxb.20200204109
5. Liu YH, Sun H, Wang JQ et al (2020) Preparation of TiO_2/MIL-88B(Fe)/polypropylene composite melt-blown nonwovens and study on dye degradation properties. J Text Res 41(2):95–102. https://doi.org/10.13475/j.fzxb.20190504808
6. Štefečka M, Kando M, Matsuo H et al (2004) Electromagnetic shielding efficiency of plasma treated and electroless metal plated polypropylene nonwoven fabrics. J Mater Sci 39(6):2215–2217. https://doi.org/10.1023/B:JMSC.0000017791.10620.e2
7. Jin KL, Kim SS, Xu J et al (2018) Melt-blown cross-linked fibers from thermally reversible Diels-Alder polymer networks. ACS Macro Lett 7(11):1339–1345. https://doi.org/10.1021/acsmacrolett.8b00685
8. Aragaw TA (2020) Surgical face masks as a potential source for microplastic pollution in the COVID-19 scenario. Mar Pollut Bull 159
9. Sójka-Ledakowicz J, Łatwińska M, Kudzin M et al (2014) A study on obtaining nonwovens using polyhydroxyalkanoates and the melt-blown technique. e-Polymers 14(5): 373–380. https://doi.org/10.1515/epoly-2014-0089
10. Wang Z, An CJ, Chen XJ et al (2021) Disposable masks release microplastics to the aqueous environment with exacerbation by natural weathering. J Hazard Mater 417:126036. https://doi.org/10.1016/j.jhazmat.2021.126036
11. Zhang JF, Chen GJ, Bhat GS et al (2020) Electret characteristics of melt-blown polylactic acid fabrics for air filtration application. J Appl Polym Sci 137:48309. https://doi.org/10.1002/app.48309
12. Vadas D, Kmetykó D, Marosi G et al (2018) Application of melt-blown Poly (lactic acid) fibres in self-reinforced composites. Polymers 10(7):766. https://doi.org/10.3390/polym10070766
13. Dzierzkowska E, Scisłowska-Czarnecka A, Kudzin M et al (2021) Effects of process parameters on structure and properties of melt-blown poly (lactic acid) nonwovens for skin regeneration. J Functio Biomater 12(1):16. https://doi.org/10.3390/jfb12010016
14. Feng JY (2017) Preparation and properties of poly(lactic acid) fiber melt blown non-woven disordered mats. Mater Lett 189:180–183. https://doi.org/10.1016/j.matlet.2016.12.013
15. Hammonds RL, Gazzola WH, Benson RS (2014) Physical and thermal characterization of polylactic acid meltblown nonwovens. J Appl Polym Sci 131(15):40593. https://doi.org/10.1002/app.40593
16. Łatwińska M, Sójka-Ledakowicz J, Chruściel J et al (2016) PLA and PP composite nonwoven with antimicrobial activity for filtration applications. Int J Polym Sci 2016:2510372. https://doi.org/10.1155/2016/2510372
17. Hernández-Alamilla M, Valadez-Gonzalez A (2016) The effect of two commercial melt strength enhancer additives on the thermal,

rheological and morphological properties of polylactide. J Polym Eng 36(1):31–41. https://doi.org/10.1515/polyeng-2014-0322
18. Narmon AS, Dewaele A, Bruyninckx K et al (2021) Boosting PLA melt strength by controlling the chirality of co-monomer incorporation. Chem Sci 12(15):5672–5681. https://doi.org/10.1039/d1sc00040c
19. Sheng XX, Zhao YF, Zhang L et al (2019) Properties of two-dimensional Ti_3C_2 MXene/thermoplastic polyurethane nanocomposites with effective reinforcement via melt blending. Compos Sci Technol 181:107710. https://doi.org/10.1016/j.compscitech.2019.107710
20. Ai X, Li X, Yu YL et al (2019) The mechanical, thermal, rheological and morphological properties of PLA/PBAT blown films by using bis(tert-butyl dioxy isopropyl) benzene as crosslinking agent. Polym Eng Sci 59(S1):E227–E236. https://doi.org/10.1002/pen.24927
21. Zhu FC, Su JJ, Wang MJ et al (2020) Study on dual-monomer melt-grafted poly(lactic acid) compatibilized poly(lactic acid)/polyamide 11 blends and toughened melt-blown nonwovens. J Ind Text 49(6):748–772. https://doi.org/10.1177/1528083718795913
22. Hu XY, Su TT, Li P et al (2018) Blending modification of PBS/PLA and its enzymatic degradation. Polym Bull 75(2):533–546. https://doi.org/10.1007/s00289-017-2054-7
23. Wang B, Hina K, Zou HT et al (2018) Thermal, crystallization, mechanical and decomposition properties of poly(lactic acid) plasticized with poly(ethylene glycol). J Vinyl Add Tech 24:E154–E163. https://doi.org/10.1002/vnl.21619
24. Jiang YP, Yan C, Shi DW et al (2019) Enhanced rheological properties of PLLA with a purpose-designed PDLA-b-PEG-b-PDLA triblock copolymer and the application in the film blowing process to acquire biodegradable PLLA films. ACS Omega 4(8):13295–13302. https://doi.org/10.1021/acsomega.9b01470
25. Li Y, Han CY, Yu YC et al (2018) Crystallization behaviors of poly(lactic acid) composites fabricated using functionalized eggshell powder and poly(ethylene glycol). Thermochim Acta 663:67–76. https://doi.org/10.1016/j.tca.2018.03.011
26. Sharma S, Singh AA, Majumdar A et al (2019) Tailoring the mechanical and thermal properties of polylactic acid-based bionanocomposite films using halloysite nanotubes and polyethylene glycol by solvent casting process. J Mater Sci 54(12):8971–8983. https://doi.org/10.1007/s10853-019-03521-9
27. Jiang YP, Yan C, Wang K et al (2019) Super-toughed PLA blown film with enhanced gas barrier property available for packaging and agricultural applications. Materials 12(10):1663. https://doi.org/10.3390/ma12101663
28. Huang HC, Chen LJ, Song GL et al (2018) An efficient plasticization method for poly(lactic acid) using combination of liquid-state and solid-state plasticizers. J Appl Polym Sci 135(36):46669. https://doi.org/10.1002/app.46669
29. Zhang CM, Lan QF, Zhai TL et al (2018) Melt crystallization behavior and crystalline morphology of polylactide/poly(epsilon-caprolactone) blends compatibilized by lactide-caprolactone copolymer. Polymers 10(11):1181. https://doi.org/10.3390/polym10111181
30. Shazleen SS, Ng LYF, Ibrahim NA et al (2021) Combined effects of cellulose nanofiber nucleation and maleated polylactic acid compatibilization on the crystallization kinetic and mechanical properties of polylactic acid nanocomposite. Polymers 13(19):3226. https://doi.org/10.3390/polym13193226
31. Tang WD, He GJ, Huang WT et al (2021) The reactive compatibilization of PLA/PP blends and improvement of PLA crystallization properties induced by in situ UV irradiation. Cryst Eng Comm 23(4):864–875. https://doi.org/10.1039/d0ce01445a
32. Jia SK, Yu DM, Wang Z et al (2019) Morphologies, crystallization, and mechanical properties of PLA-based nanocomposites: Synergistic effects of PEG/HNTs. J Appl Polym Sci 136(18):47385. https://doi.org/10.1002/app.47385
33. Zhu FC, Yu B, Su JJ et al (2020) Study on PLA/PA11 bio-based toughening melt-blown nonwovens. Autex Res J 20(1):24–31. https://doi.org/10.2478/aut-2019-0002
34. Ozdemir E, Hacaloglu J (2018) Thermal degradation of Polylactide/Poly(ethylene glycol) fibers and composite fibers involving organoclay. J Anal Appl Pyrol 129:181–188. https://doi.org/10.1016/j.jaap.2017.11.014
35. Jarecki L, Ziabicki A, Lewandowski Z et al (2011) Dynamics of air drawing in the melt blowing of nonwovens from isotactic polypropylene by computer modeling. J Appl Polym Sci 119(1):53–65. https://doi.org/10.1002/app.31973
36. Peng MN, Jia HY, Jiang L et al (2019) Study on structure and property of PP/TPU melt-blown nonwovens. J Text Inst 110(3):468–475. https://doi.org/10.1080/00405000.2018.1485461
37. Cespi M, Bonacucina G, Tiboni M et al (2021) Insights in the rheological properties of PLGA-PEG-PLGA aqueous dispersions: structural properties and temperature-dependent behaviour. Polymer 213:123216. https://doi.org/10.1016/j.polymer.2020.123216
38. Nazari T, Garmabi H (2018) The effects of processing parameters on the morphology of PLA/PEG melt electrospun fibers. Polym Int 67(2):178–188. https://doi.org/10.1002/pi.5486
39. Nazari T, Garmabi H (2016) Thermo-rheological and interfacial properties of polylactic acid/polyethylene glycol blends toward the melt electrospinning ability. J Appl Polym Sci 133(44):44120. https://doi.org/10.1002/app.44120
40. Mohapatra AK, Mohanty S, Nayak SK (2016) Properties and characterization of biodegradable poly(lactic acid) (PLA)/poly(ethylene glycol) (PEG) and PLA/PEG/organoclay: A study of crystallization kinetics, rheology, and compostability. J Thermoplast Compos Mater 29(4):443–463. https://doi.org/10.1177/0892705713518812
41. Pan N, Lin C, Xu J (2019) A new method for measuring fabric drape with a novel parameter for classifying fabrics. Fibers 7(8):70. https://doi.org/10.3390/fib7080070